Available online at www.sciencedirect.com
ScienceDirect
Journal of the European Ceramic Society 30 (2010) 2849–2857
www.elsevier.com/locate/jeurceramsoc

Micellar layer-by-layer synthesis of TiO_2/Ag hybrid particles for bactericidal and photocatalytic activities

Wei-Cheng Lin [a], Chun-Nan Chen [a], Tzu-Tsung Tseng [a], Ming-Hsiung Wei [b], J.H. Hsieh [c], Wenjea J. Tseng [a,*]

[a] *Department of Materials Science and Engineering, National Chung Hsing University, 250 Kuo Kuang Road, Taichung 402, Taiwan*
[b] *Chung-Shan Institute of Science and Technology, Taoyuan, Taiwan*
[c] *Department of Materials Engineering, Mingchi University of Technology, 84 Gungjuan Rd., Taishan, Taipei 243, Taiwan*

Available online 13 January 2010

Abstract

Silver nanoparticles prepared by a reverse micelle process were sequentially deposited on rutile-structured TiO_2 particles via an electrostatic layer-by-layer (LbL) deposition together with a hydrophilic/hydrophobic interaction. The TiO_2 surface was first mediated by a preferential adsorption of poly(allylamine hydrochloride) (PAH) cationic molecules, before being mixed with the Ag nanoparticles encapsulated in reverse micelles consisting of anionic surfactant of sodium bis(2-ethylhexyl) sulfosuccinate (AOT) in isooctane. The deposition of Ag nanoparticles was not of a uniform coverage on the TiO_2 surface, but of a heterogeneous growth of the Ag particles on the TiO_2 surface. Antibacterial activity of the composites against gram-negative bacteria, i.e., *Escherichia coli* (*E. coli*), was found to increase with the deposition cycle, resulted mainly from the increased Ag concentration. The bactericidity is persistent in the absence of ultraviolet (UV) light. Over the concentration range of Ag examined, i.e., Ag/Ti atomic ratio varies from 0.28% to 0.53%, photocatalytic efficiency of the composites against methylene blue (MB) dye in an aqueous solution also improved pronouncedly with the silver concentration under UV exposure.

Keywords: TiO_2; Ag; Composite; Antibacterial; Photocatalysis

1. Introduction

An imminent need for meeting the energy and environmental challenges has led to a recurrent interest on titanium dioxide (TiO_2); to which, many of the applications rely not only on the property of the semi-conductive TiO_2 material itself but also on the modification of the TiO_2 as a host material.[1–3] Crystalline TiO_2 with anatase or rutile structure has been regarded by many as an efficient and environmentally benign photocatalyst, and has been widely used for photodegradation of various pollutants and for bactericidal material as well.[3–8] On the other hand, silver (Ag) nanoparticles have long been known to liberate silver ions in liquids that show a broad spectrum over the antimicrobial activities.[9,10] Immobilization of Ag nanoparticles on TiO_2 to form hybrid composite particles with tailored structure and surface functionality has been demonstrated to show improved photocatalytic activity,[3,11–13] as well as bactericidal activity[14–16] without the need of UV irradiation.

Considerable success has been achieved recently in terms of the variety of well-defined composite structure and the versatility of the synthesis process. In view of the literature,[11–14,16] preparation of the hybrid TiO_2/Ag particles often involves a preferential deposition of silver nuclei followed then by the growth of silver layer, or by a direct coating from the silver nanoparticles on surface of TiO_2 with a specific surface modification prior the silver deposition. A wide range of wet chemical routes has been reported, including electrostatic layer-by-layer (LbL) deposition, surface chemical reaction, photochemical reduction, polyol process, ultrasonic electrodeposition, and soft template process.[11–14,16–20] For the heterogeneous nucleation and growth of silver shell on TiO_2 particles, surface pre-treatment is required in order to facilitate formation of effective chemical bonding sites on the TiO_2 surface before the Ag shell can be formed. The surface modification becomes indispensable when vitreophobic aggregation of the metallic Ag needs to be suppressed. The LbL method,[20] on the other hand, provides an alternative route for the synthesis of heterogeneous composite particles or hollow particles by consecutive nanoparticle deposition on the core surface via an electrostatic layer-by-layer process scheme. This process readily affords control over the multilayer build up so that

* Corresponding author.
E-mail address: wenjea@dragon.nchu.edu.tw (W.J. Tseng).

0955-2219/$ – see front matter © 2009 Elsevier Ltd. All rights reserved.
doi:10.1016/j.jeurceramsoc.2009.12.016

the concentration of shell material can be manipulated through change of coating numbers for the nanoparticle deposition. Metallic Ag particles often bear a negative surface charge over a broad pH range,[21] so as the TiO_2. This creates some difficulties in the LbL process since both the targeted core material and the shell material present a net surface charge of the same sign over the working pH employed. The problem may be solved by adsorption of polyelectrolyte molecules on the TiO_2 surface that changes the surface polarity. In this regard, Lu and co-workers[22] recently proposed a reverse micellar nanoparticle-based process that features an additional hydrophilic/hydrophobic interaction to facilitate the nanoparticle build up in addition to the electrostatic attraction used in the LbL method. The proposed method stabilized the metal shell by addition of an anionic AOT surfactant molecule that forms reverse micelles in organic solvent to encapsulate the metallic nanoparticles; whilst, the surface of oxide core was mediated by a cationic PAH polyelectrolyte in water. When the PAH-modified TiO_2 particles are added into the silver suspensions stabilized with the AOT micelles in given non-polar solvent, heterogeneous adsorption is rendered by the hydrophilic/hydrophobic interaction together with the electrostatic attraction in facilitating the nanoparticle deposition.

Despite the reverse micellar LbL process was conducted successfully on synthesis of several core–shell composite and hollow particles,[22] extension of the process to the synthesis of TiO_2/Ag hybrids and the detailed structural characterization and property evaluation have not been explored. In this study, the reverse micellar LbL process was conducted for the synthesis of TiO_2/Ag composite, and the resulting composite structure was characterized by zeta potential, SEM-EDS, TEM, XRD, ESCA, and ICP analysis, respectively, upon completion of every adsorption cycle. Up to five coating cycles were examined. Antibacterial activity against *E. coli* and photocatalytic efficiency against MB dye were carried out in aqueous liquids as the adsorption cycle varies.

2. Experimental details

2.1. Materials

TiO_2 particles (Wanyuan Technology Co., Taiwan) with an average diameter of 280 nm, purity >95%, and a B.E.T. surface area of 13 m^2/g were used as the starting material. The particles are about spherical in shape (Fig. 1) and are of rutile phase in structure. Reagent-grade silver nitrate ($AgNO_3$, 99.7 wt.%, J.T. Baker, USA), ethanol (EtOH, Fluka, Switzerland), ammonia solution (NH_4OH, 28 wt.% NH_3 in water, Osaka Chemical, Japan), sodium chloride (NaCl, 99.8%, Riedelde Haën, Germany), sodium bis(2-ethylhexyl) sulfosuccinate (AOT, $C_{20}H_{37}NaO_7S$, 98%, Alfa, USA), sodium borohydride ($NaBH_4$, Riedelde Haën, Germany), and poly(allylamine hydrochloride) (PAH, MW ~60,000, Alfa, USA) were purchased commercially and used without further purification. De-ionized water (18.2 MΩ) was from a Millipore Milli Q filtration system. *E. coli* was obtained from the American Type Culture Collection.

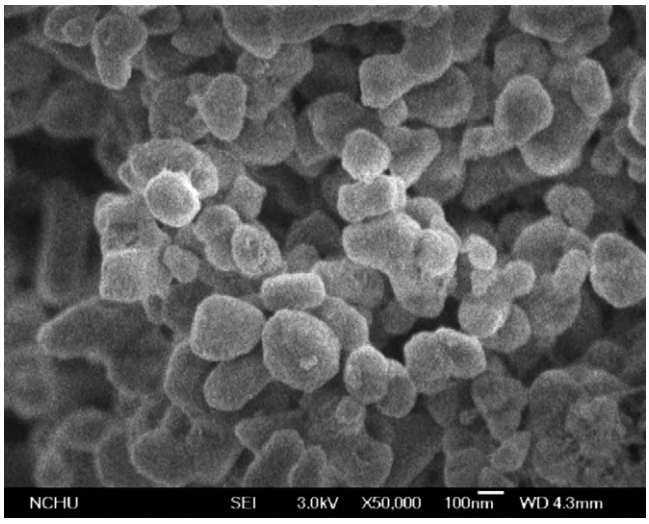

Fig. 1. Particle morphology of the as-received TiO_2 particles.

Methylene blue dye ($C_{16}H_{18}ClN_3S{\cdot}3H_2O$, MW ~ 374) was purchased from Unilab Industries (Taiwan), and was diluted before use.

2.2. Synthesis

The TiO_2 particles of 0.2 g were dispersed in PAH solution consisting of 0.1 g PAH dissolved in 100 ml of 0.5 M NaCl aqueous solution. The solution pH was held at about 7.2, and the colloidal solution was magnetically stirred for 30 min, followed then by collection of the surface-mediated particles through centrifuge. Reverse micellar synthesis of silver nanoparticle was obtained from mixing of two ionic solutions. One of the solutions consists of 0.034 g $AgNO_3$ dissolved in isooctane–water mixture (49.1 and 0.9 ml, respectively) with 2.175 g AOT (equivalent to 0.1 M). The $AgNO_3$ serves as the precursor for the Ag nanoparticles. The other solution containing the reducing agent for silver was prepared similarly by mixing 0.038 g $NaBH_4$ in the AOT-added isooctane–water mixtures. Nanometer-sized Ag particles were formed by mixing the two ionic solutions under vigorous stirring at 25 °C for 30 min, and the nanoparticles were stabilized by the reverse micelles formed by the AOT molecules.

The TiO_2/Ag hybrid particles were prepared by slowly redispersing the PAH-mediated TiO_2 particles in the Ag-containing AOT micellar solution with a continuous magnetic stirring for 30 min. The particles were then centrifuged, rinsed in ethanol repeatedly for three times to complete one adsorption cycle. Multiple Ag depositions were prepared by repeating the mixing of the PAH-modified composite particles with the Ag-containing AOT micellar solution, followed then by the same centrifuge and rinse process to remove the loosely anchored surfactant molecules and Ag nanoparticles. Up to five deposition cycles were performed in the study, and the resulting TiO_2/Ag composite particles were calcined at 400 °C in ambient air to remove the low-melting organic surfactants and solvents.

2.3. Characterization

Zeta potential (ζ potential) of the TiO_2 and the TiO_2/Ag hybrid particles was determined by a dynamic light-scattering spectroscopy (Zetasizer NS, Malvern Instruments, UK). The pH was adjusted with HNO_3 and NH_4OH. Particle morphology and composite structure were examined by field-emission scanning electron microscopy (FE-SEM, JSM-6700F, JEOL, Japan) equipped with an energy-dispersive spectroscopy (EDS, Oxford Inca Energy 400, UK), and by transmission electron microscopy (TEM, JEM-2010, JEOL, Japan). Structure of the composite particles was characterized by X-ray diffractometry (XRD, MAC MXP III, Japan) using Cu Kα radiation with a characteristic wavelength of 1.5406 Å. Elemental distribution of the composite particles was examined by field-emission electron spectroscopy for chemical analysis (ESCA/Auger, ULVAC-PHI, PHI 5000 VersaProbe, Japan). The samples were prepared by first mixing the particles in ethanol via ultrasonication. A few drops of the dispersions were then placed onto an electrically conductive glass plate by a pipette before being dried ready for the analysis. Chemical composition of the particles was determined semi-quantitatively by EDS-ZAF analysis, and more precisely, by an inductively coupled plasma atomic emission spectrometer (ICP-AES, ICAP 9000, Jarrell-Ash, USA).

2.4. Bactericidal activity

The antibacterial activity of the TiO_2/Ag composites with either one or three adsorption cycles was conducted against *E. coli* by the plate-counting method.[23] The particles of 1 mg were weighed precisely and added into 7 ml of a phosphate buffer solution containing the bacteria. The powdered solutions (pH ~ 7.5) were incubated at 37 °C under vibration agitation for up to 24 h. Some of the solutions (0.5 ml) were then cultured on an agar plate and incubated at 37 °C for additional 17 h, and the exact number of discrete colonies was counted as the number of remaining bacteria. A parallel test of the TiO_2 particles without the Ag adsorption was conducted for comparison purposes. The bactericidal efficiency (R) was determined by the reduction of bacteria, i.e.

$$R\ (\%) = \frac{A - B}{A} \times 100 \quad (1)$$

where R is the ratio of bacterial reduction, A is the number of bacterial colonies from the particulate solution without Ag, and B is the number of bacterial colonies from the TiO_2/Ag solution treated by different periods of isothermal incubation.

2.5. Photocatalytic activity

The photocatalytic experiment was conducted in aqueous solution with UV irradiation time up to 90 min. Solids loading of the TiO_2/Ag-containing solutions were held at 50 mg/L, while the initial concentration of the aqueous MB dye was at 5×10^{-6} M. Prior the test, all the suspensions were kept in darkness for 10 min to establish an adsorption–desorption equilibrium. Analytical samples were siphoned out from the reaction suspensions after different reaction times and then centrifuged to separate the particles from the solutions. The solutions were then characterized by an UV–vis spectrometer (Lambda 800, Perkin-Elmer, USA) to determine the absorption change over a range of wavelength from 200 to 900 nm. The residual MB concentration was determined from the absorption change using a 3-point calibration curve.

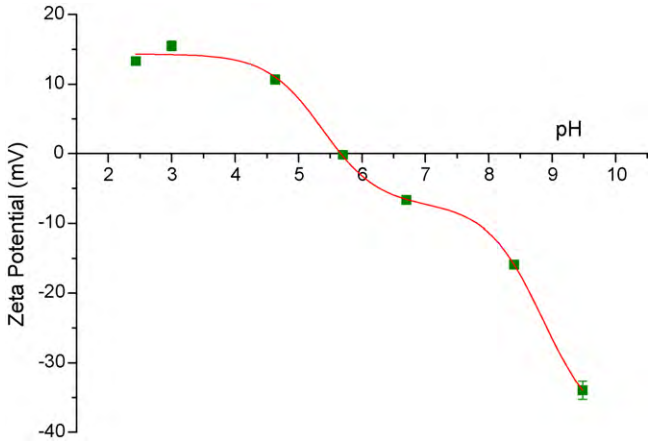

Fig. 2. Zeta potential varies with solution pH for the as-received TiO_2 particles.

3. Results and discussion

3.1. TiO_2/Ag hybrid structure and composition

Fig. 2 shows ζ potential of the as-received TiO_2 particles. The isoelectrical point (IEP) occurs at pH ~ 5.5. Solution pH used in the study was at about 7.2, the TiO_2 particles hence bear a negative surface charge. In Fig. 3, the surface potential changes pronouncedly from negative to positive, i.e., ζ potential increases from −12 to +48 mV, when PAH molecules were adsorbed on the TiO_2 surface. This surface charge promotes preferential adsorp-

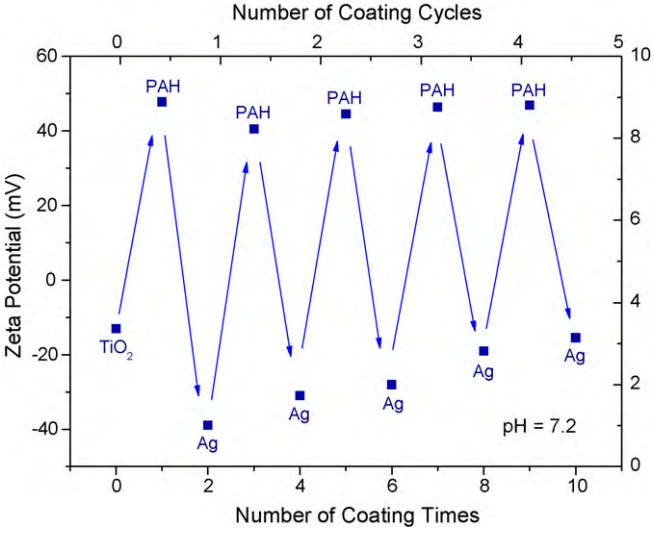

Fig. 3. Cyclic ζ-potential profile of the hybrid particles occurs when the deposition of PAH molecules and AOT-encapsulated Ag nanoparticles were conducted sequentially.

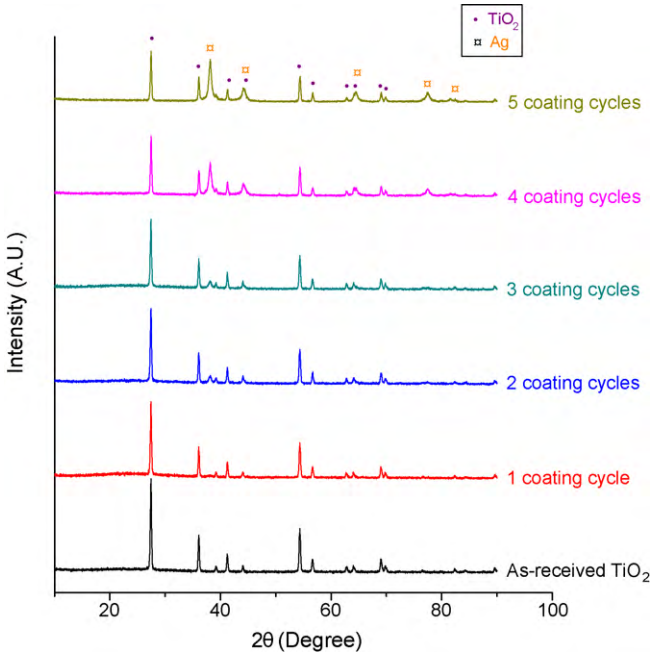

Fig. 4. XRD patterns for the TiO_2/Ag hybrid particles with various deposition cycles.

tion of the Ag nanoparticles (negative ζ potential)[21] on the PAH-modified TiO_2 (positive ζ potential) in isooctane solvent by both electrostatic attraction and hydrophilic/hydrophobic interaction.[22] The silver adsorption is confirmed by the shift of ζ potential accordingly, i.e., from +48 mV to −39 mV, upon completion of one adsorption cycle. Further repeating the deposition process shows a cyclic ζ potential change on the composite surface, revealing that the multiple Ag adsorptions occurred as the deposition process proceeds.

X-ray analysis confirms the Ag deposition on TiO_2 particles (Fig. 4). Diffraction intensities from the Ag crystallites appear to increase with the deposition cycle, indicating that Ag content in the composites increased with the number of deposition. From ESCA chemical analysis, a wide scan in binding energy showed peaks ascribed to elements of O 1s, Ti 2p, and Ag 3d. A high resolution scan of the Ti 2p region shows $2p_{1/2}$ and $2p_{2/3}$ signals in Fig. 5a. When compared to that of the as-received TiO_2 particles, only minor shift toward higher binding energies was found for that of the TiO_2/Ag hybrid particles, suggesting that no significant chemical interaction occurred for the TiO_2/Ag hybrid particles with the Ag deposition. The O 1s peak shown in Fig. 5b at binding energy of 533.0–533.6 eV corresponds to O bound to H (532.8 eV).[15] This indicates that the hydroxide bonding occurred at the surface of both TiO_2 and TiO_2/Ag particles, wherein the OH groups are thought to be mainly chemisorbed to the particle surface.[16] Nonetheless, a slight peak broadening and a shoulder over the lower energy side of the O 1s signal reveal that minor O–Ti^{4+} bond (530.2 eV)[15] may exist within the typical effective penetration depth of the ESCA analysis (~5 nm). In addition, a high resolution scan of the Ag 3d region (Fig. 5c) show peaks of $3d_{5/2}$ and $3d_{3/2}$ at 369.2 and 375.2 eV for the TiO_2/Ag composites, respectively. The binding energies were in good agreement with those of TiO_2/Ag films

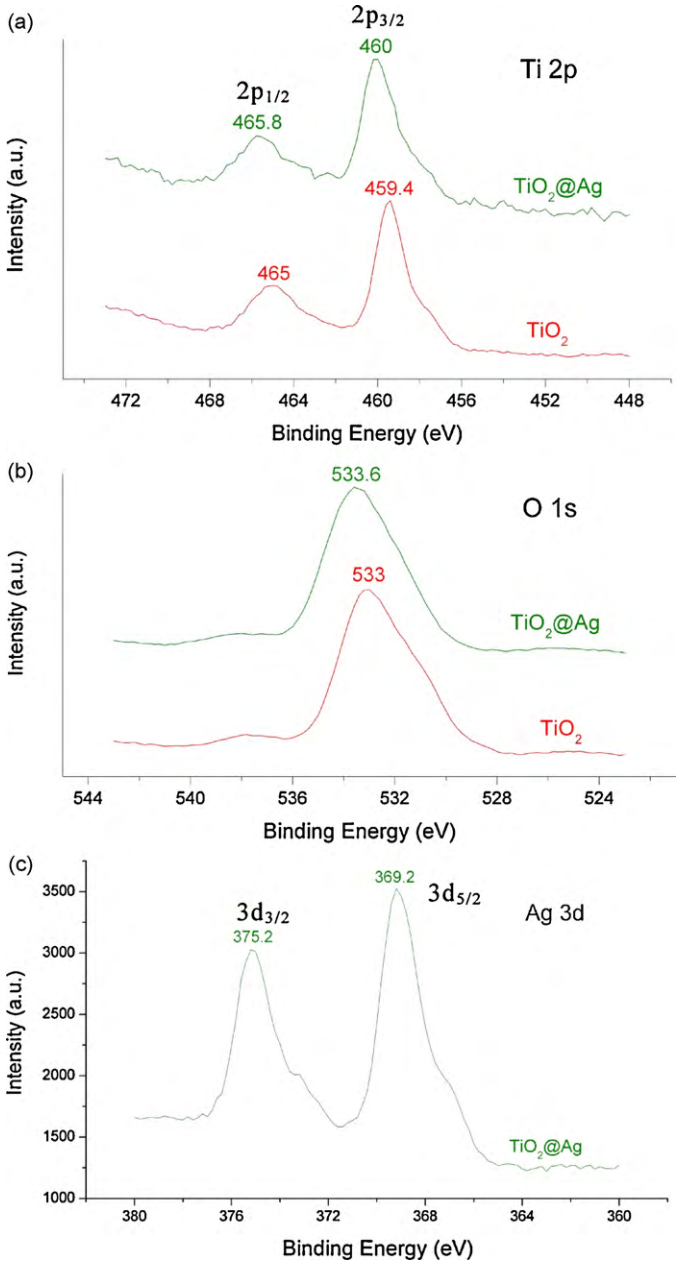

Fig. 5. The binding energy spectrum of ESCA for TiO_2/Ag hybrid particles with 3 deposition cycles.

reported elsewhere,[15,16] indicating that metallic silver was the major phase in the composite and the interactions between TiO_2 and Ag was also negligible. However, deconvolution of the Ag $3d_{5/2}$ peak yields two peak maxima, one lying at a very similar energy to that of pure Ag, i.e., 369.2 eV, while the other one is located at a lower energy of 367.1 eV. According to the literature,[11,24] this peak may be attributed to silver oxide, i.e., Ag_2O with $3d_{5/2}$ energy at 367.8 eV or AgO with $3d_{5/2}$ energy at 367.4 eV, or even both. This hence indicates that some silver oxide may exist as a minor phase in the composites.

Fig. 6 shows typical hybrid microstructures in secondary electron and backscattered scanning electron images, respectively. The primary Ag particles present a mean diameter less

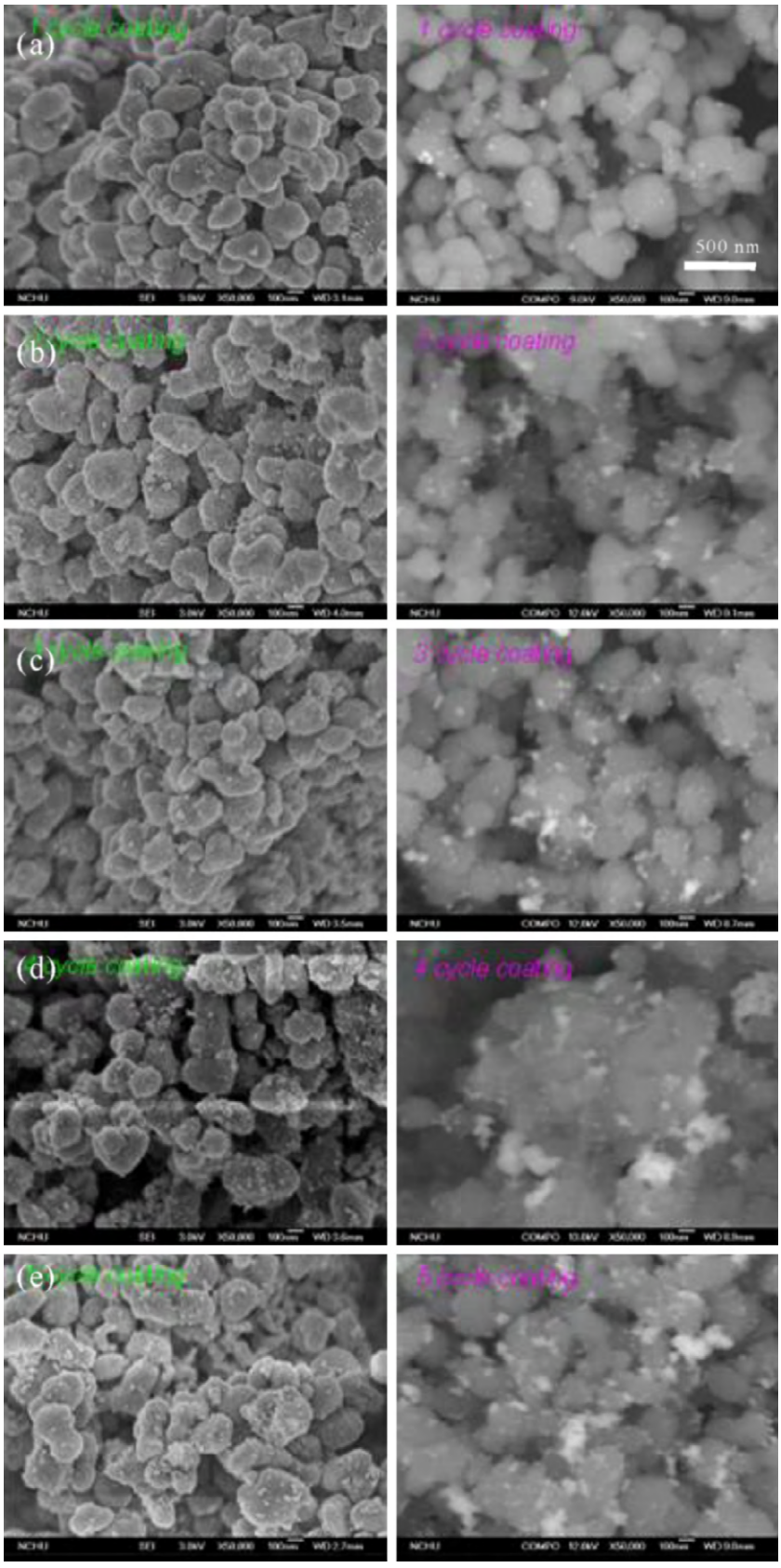

Fig. 6. SEM micrographs of the TiO_2/Ag hybrid particles with (a) one, (b) two, (c) three, (d) four, and (e) five deposition cycles, respectively. (Left: secondary electron image, Right: backscattered electron image.)

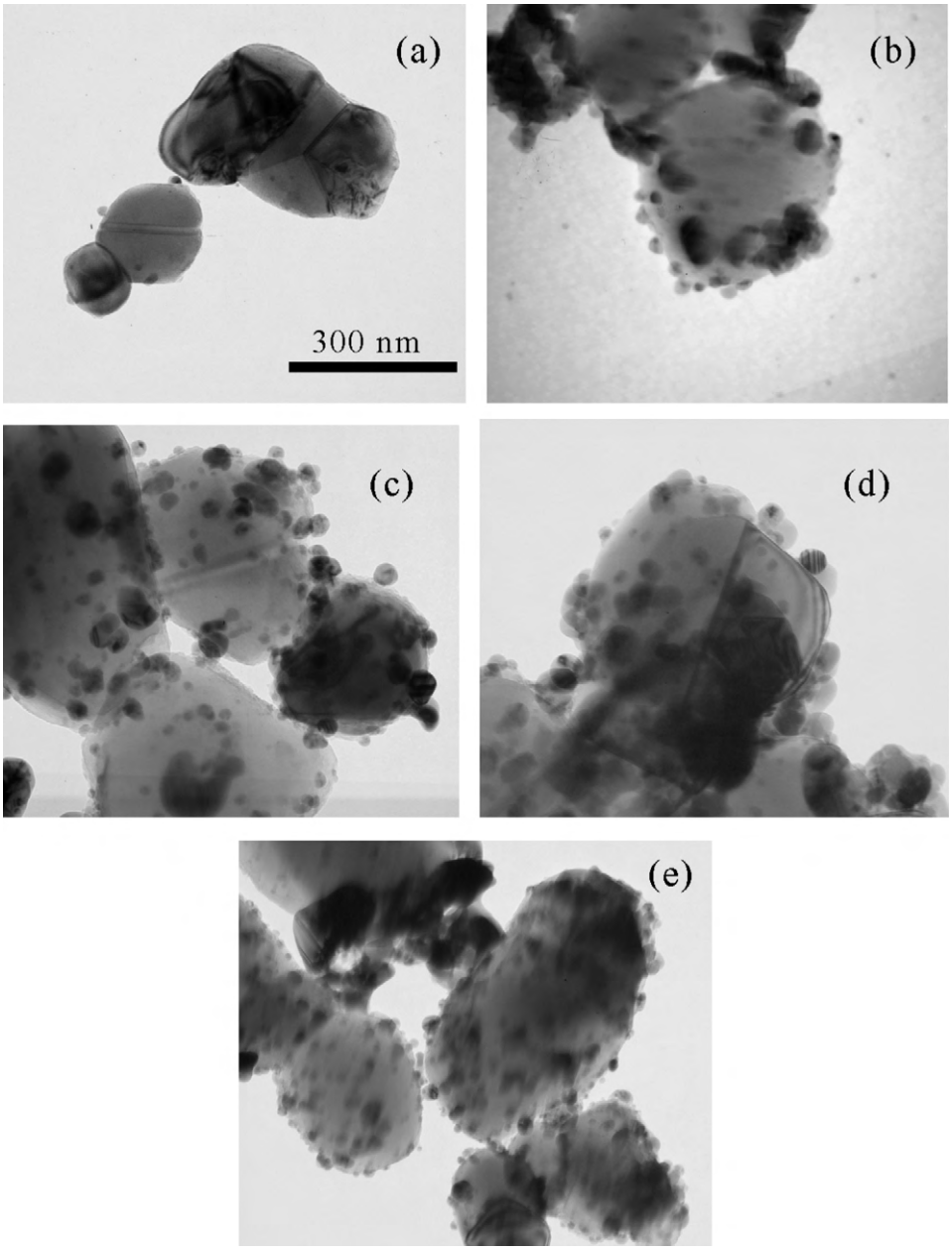

Fig. 7. Bright-field TEM micrographs of the TiO_2/Ag hybrid particles with (a) one, (b) two, (c) three, (d) four, and (e) five deposition cycles, respectively.

than 10 nm, and are easily distinguishable from the submicrometer TiO_2 particles. Distribution of the Ag nanoparticles appears to be scattered on the TiO_2 surface, instead of forming a complete coverage layer around the TiO_2 particles. This becomes more apparent from the backscattered images, since the high Z silver scatters more electrons. In addition, the nanoparticle-based heterogeneous adsorption occurred for all deposition cycles examined; in particular, the growth of Ag aggregates appeared to become more pronounced as the deposition cycles increases. Even though a uniform core–shell structure was not obtained, the Ag coverage apparently increases, so as its concentration, with the multiple depositions. From EDS-ZAF analyses, the Ag concentration increased linearly with the deposition cycle. The build up of Ag nanoparticles on the TiO_2 particles is also shown in Fig. 7 by TEM examinations. The Ag nanoparticles were seen to adsorb preferentially on the TiO_2 surface; to which, the Ag particles appeared to adhere exclusively on the PAH-modified TiO_2 surface. Therefore, "free" Ag nanoparticles not anchoring with the TiO_2 were not found from the TEM examinations. In addition, the Ag nanoparticles favoured to form spherical aggregates with diameter as large as 50 nm, rather than formation of a nanoparticle monolayer around the TiO_2 particle. This reveals a stronger interparticle attraction between the neighbouring Ag particles than that of the heterogeneous electrostatic attraction over the PAH-modified TiO_2 surface sites and the electronegative Ag surface.

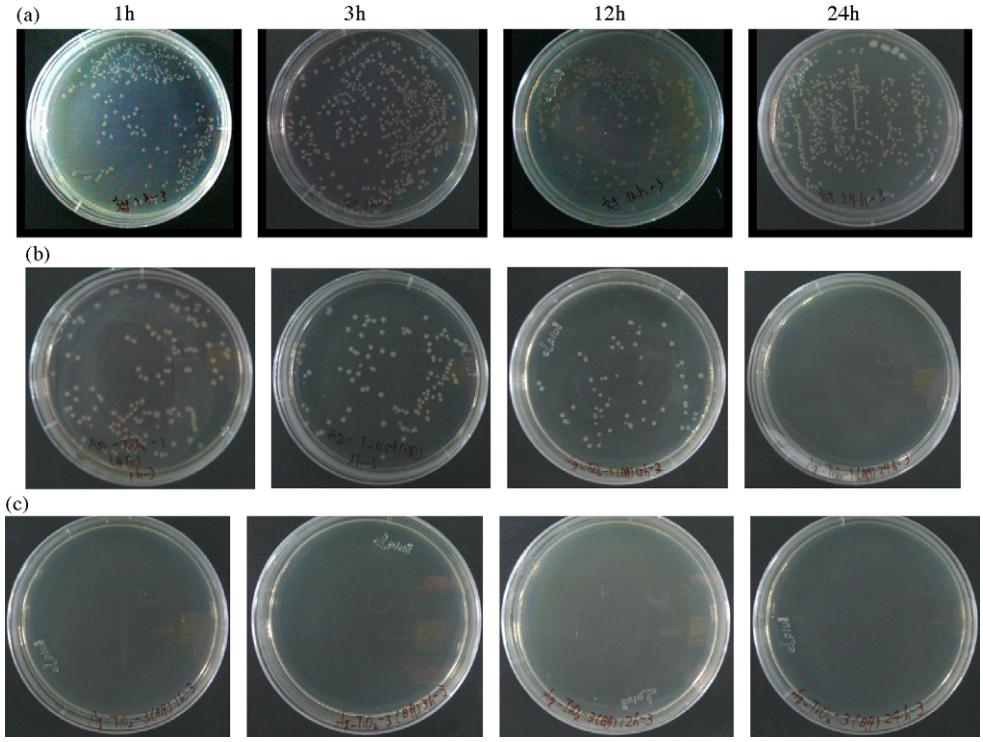

Fig. 8. Photographs of the plate-counting antibacterial results for the TiO_2/Ag hybrid particles on *E. coli* after a range of immersion times (1–24 h). (a) TiO_2 particles without Ag adsoprtion, (b) TiO_2/Ag hybrid particles with 1 coating cycle, and (c) with 3 coating cycles.

3.2. Antibacterial activity

The bactericidal effect of the TiO_2/Ag composites against *E. coli* has been conducted by the plate-counting method both with and without the UV exposure for various incubation times (1–24 h) at 37 °C. A parallel test of the as-received TiO_2 particles without the silver adsorption has also been carried out for comparisons. With the UV irradiation, the TiO_2 particles without Ag did not show much of the bactericidal effect over the incubation times examined (Fig. 8a). For the plates containing the composites with one adsorption cycle, a notable reduction of the gram-negative *E. coli* occurs after 12 h of incubation, and extinction of the *E. coli* happens upon extension of the duration to 24 h (Fig. 8b). In comparison, the bacterial colonies were completely not seen within merely 1 h duration for the TiO_2/Ag composites with three adsorption cycles (Fig. 8c). In addition, the bactericidal property remains when the incubation duration extends to 24 h.

The percentage of bacterial reduction upon UV illumination is shown in Fig. 9. The bactericidal efficiency (R) increases slowly from ca. 45% to >99% as the incubation time increases from 1 to 12 h for the composites with one adsorption cycle. On the other hand, R increases rapidly to reach >99% after 1 h duration for the TiO_2/Ag composites with three adsorption cycles. The bactericidity persists when the incubation duration was prolonged to 24 h. According to ICP-AES analyses, silver concentration in the composites increases from 1399 to 2359 ppm, corresponding equivalently to an Ag/Ti atomic ratio from 0.25% to 0.53%, as the deposition cycle increases from one to three. Estimate of the silver concentration, by assuming that only metallic silver exists, falls in the range of 0.168–0.316 wt.% for the hybrid composites. This indicates that the composite particles can release Ag ions in a sufficient concentration to kill the *E. coli* effectively even though the Ag content is only moderate.[16,25]

Without the UV irradiation, the bactericidity of the hybrid composites still remains effective. Identical to that of the composites with UV exposure, R increases rapidly to reach >99% after 1 h incubation and remains bacteria-free upon extension to 24 h in the absence of UV for the composites with three Ag adsorptions. Similarly, the composite particles with one silver

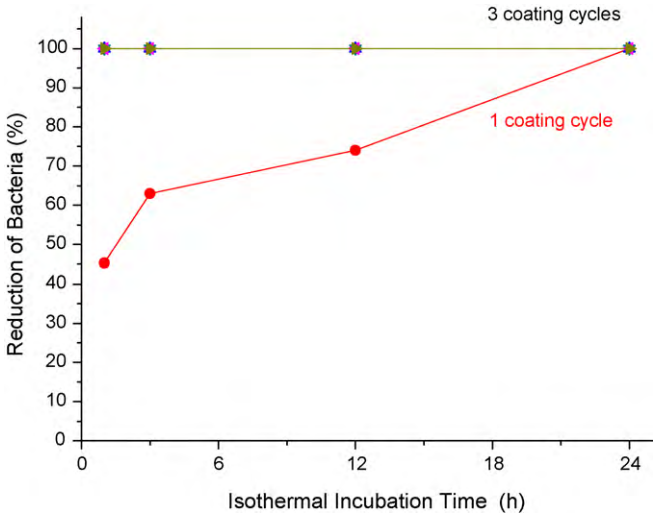

Fig. 9. Reduction of *E. coli* over 1–24 h of isothermal incubation.

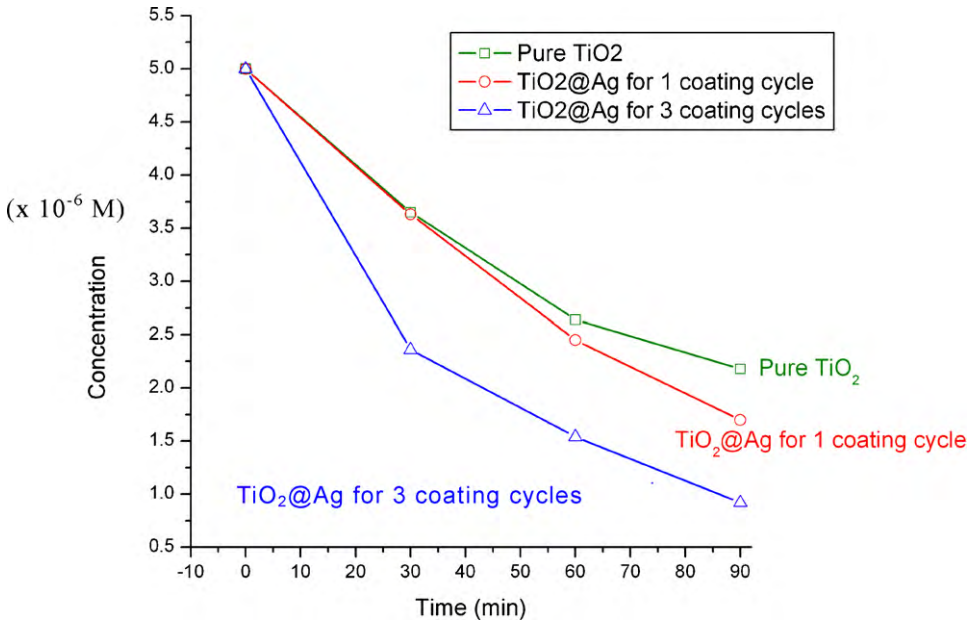

Fig. 10. Photodegradation of MB dye solution under UV irradiation.

adsorption show a bactericidal efficiency of 51% upon 1 h duration of incubation. The bacterial reduction then reaches 95% when prolonging to 3 h of incubation, before finally becomes >99% upon extension to 12 h. Therefore, the TiO_2/Ag composite particles show bactericidal property in both with and without the UV irradiation. The difference in the bactericidal performance stems mainly from the silver concentration of the composite particles.

3.3. Photocatalytic property

The concentration of aqueous MB dye solution reduces with the UV irradiation, as shown in Fig. 10. The photocatalysis mechanism involves adsorption of MB dye molecules in water on the surface of TiO_2 particles, which are then excited by the UV energy to generate the electron and hole pairs within the particle volume. The electron–hole pairs would migrate to the particle surface and serve as redox sites for the deconstruction of the surface adsorbed dye molecules.[11] In Fig. 10, the photocatalytic activity is enhanced by the presence of silver nanoparticles. The photodegradation of MB dye with increased efficiencies up to 63% (MB concentration from 2.4 to 0.9 μM) and 29% (MB concentration from 2.4 to 1.7 μM) is observed for the suspensions containing the TiO_2/Ag composites with adsorption cycles of three and one, respectively. Deposition of silver on TiO_2 surface has been reported to enhance the photoinduced electron/hole lifetimes as a result of effective trapping of the photoinduced electrons to the surface deposited Ag sites.[26] In addition, the MB adsorption would increase with the Ag concentration in sol–gel derived TiO_2 over a broad concentration range (0.01–10 mol.%).[11] Both are considered to govern the observed photocatalytic dependence on the Ag concentration.

4. Conclusion

Silver nanoparticles encapsulated in reverse micelles consisting of anionic surfactant of sodium bis(2-ethylhexyl) sulfosuccinate (AOT) in isooctane were sequentially deposited on rutile-structured TiO_2 particles mediated by a preferential adsorption of poly(allylamine hydrochloride) (PAH) cationic molecules by an electrostatic layer-by-layer deposition together with a hydrophilic/hydrophobic interaction. The deposition of Ag nanoparticles on the TiO_2 surface was not of a uniform coating, but of a heterogeneous growth of the scattered Ag nanoparticles specifically on the TiO_2 surface. Growth of the Ag primary particles to aggregates was observed as the deposition cycle increased. The TiO_2/Ag hybrid particles show antibacterial activity against gram-negative *E. coli* both in the presence and absence of UV irradiation. The bactericidal performance was found to increase with the Ag concentration over the moderate Ag concentration range examined, i.e., the Ag/Ti atomic ratio ranged from 0.28% to 0.53%. On the other hand, photocatalytic efficiency of the composites against methylene blue dye in aqueous solutions also improved pronouncedly (up to 63% increase) with the silver concentration examined under the UV exposure. Inhibited electron–hole recombination and increased adsorption of MB dye due to the presence of Ag nanoparticles are considered the main reasons for the enhanced photocatalysis.

Acknowledgments

Financial support from the Chung Shan Institute of Science and Technology through contract no. CSIST-800-V110(98) and from the National Science Council (Taiwan, ROC) under contract no. NSC 95-2221-E-005-036-MY3 is gratefully acknowledged.

References

1. Honda K, Fujishima A. Electrochemical photolysis of water at a semiconductor electrode. *Nature* 1972;**238**:37–8.
2. O'Regan B, Grätzel M. A low-cost, high efficiency solar cell based on dye-sensitized colloidal TiO_2 films. *Nature* 1991;**353**:737–40.
3. Chen X, Mao SS. Titanium dioxide nanomaterials: synthesis, properties, modifications, and applications. *Chem Rev* 2007;**107**:2891–959.
4. Diebold U. The surface science of titanium dioxide. *Surf Sci Rep* 2003;**48**:53–229.
5. Toma F-L, Bertrand G, Begin S, Meunier C, Barres O, Klein D, et al. Microstructure and environmental functionalities of TiO_2-supported photocatalysts obtained by suspension plasma spraying. *Appl Catal B: Environ* 2006;**68**:74–84.
6. Navarro E, Baun A, Behra R, Hartmann NB, Filser J, Miao A-J, et al. Environmental behavior and ecotoxicity of engineered nanoparticles to algae, plants, and fungi. *Ecotoxicology* 2008;**17**:372–86.
7. Li Q, Mahendra S, Lyon DY, Brunet L, Liga MV, Li D, et al. Antimicrobial nanomaterials for water disinfection and microbial control: potential applications and implications. *Water Res* 2008;**42**:4591–602.
8. Page K, Wilson M, Parkin IP. Antimicrobial surfaces and their potential in reducing the role of the inanimate environment in the incidence of hospital-acquired infections. *J Mater Chem* 2009;**19**:3819–31.
9. Kawashita M, Tsuneyama S, Miyaji F, Kokubo T, Kozuka H, Yamamoto K. Antibacterial silver-containing silica glass prepared by sol–gel method. *Biomaterials* 2000;**21**:393–8.
10. Sharma VK, Yngard RA, Lin Y. Silver nanoparticles: green synthesis and their antimicrobial activities. *Adv Colloid Interface Sci* 2009;**145**:83–96.
11. Priya R, Baiju KV, Shukla S, Biju S, Reddy MLP, Patil K, et al. Comparing ultraviolet and chemical reduction techniques for enhancing photocatalytic activity of silver oxide/silver deposited nanocrystalline anatase titania. *J Phys Chem C* 2009;**113**:6243–55.
12. Chen HW, Ku Y, Kuo YL. Photodegradation of o-cresol with Ag deposited on TiO_2 under visible and UV light irradiation. *Chem Eng Technol* 2007;**30**:1242–7.
13. Cozzoli PD, Fanizza E, Comparelli R, Curri ML, Agostiano A, Laub D. Role of metal nanoparticles in TiO_2/Ag nanocomposite-based microheterogeneous photocatalysis. *J Phys Chem B* 2004;**108**:9623–30.
14. Yang C, Liang GL, Xu KM, Gao P, Xu B. Bactericidal functionalization of wrinkle-free fabrics via covalently bonding TiO_2@Ag nanoconjugates. *J Mater Sci* 2009;**44**:1894–901.
15. Brook LA, Evans P, Foster HA, Pemble ME, Steele A, Sheel DW, et al. Highly bioactive silver and silver/titania composite films grown by chemical vapour deposition. *J Photochem Photobiol A: Chem* 2007;**187**:53–63.
16. Es-Souni M, Fischer-Brandies H, Es-Souni M. Versatile nanocomposite coatings with tunable cell adhesion and bactericidity. *Adv Funct Mater* 2008;**18**:3179–88.
17. Korzhak AV, Ermokhina NI, Stroyuk AL, Bukhtiyarov VK, Raevskaya AE, Litvin VI, et al. Photocatalytic hydrogen evolution over mesoporous TiO_2/metal nanocomposites. *J Photochem Photobiol A: Chem* 2008;**198**:126–34.
18. Cozzoli PD, Comparelli R, Fanizza E, Curri ML, Agostiano A, Laub D. Photocatalytic synthesis of silver nanoparticles stabilized by TiO_2 nanorods: a semiconductor/metal nanocomposite in homogeneous nonpolar solution. *J Am Chem Soc* 2004;**126**:3868–79.
19. Jeong U, Wang Y, Ibisate M, Xia Y. Some new developments in the synthesis, functionalization, and utilization of monodisperse colloidal spheres. *Adv Funct Mater* 2005;**15**:1907–21.
20. Wang Y, Angelatos AS, Caruso F. Template synthesis of nanostructured materials via layer-by-layer assembly. *Chem Mater* 2008;**20**:848–58.
21. Alvarez-Puebla RA, Aroca RF. Synthesis of silver nanoparticles with controllable surface charge and their application to surface-enhanced Raman scattering. *Anal Chem* 2009;**81**:2280–5.
22. Chen G-C, Kuo C-Y, Lu S-Y. A general process for preparation of core-shell particles of complete and smooth shells. *J Am Ceram Soc* 2005;**88**:277–83.
23. Wang J-X, Wen L-X, Wang Z-H, Chen J-F. Immobilization of silver on hollow silica nanospheres and nanotubes and their antibacterial effects. *Mater Chem Phys* 2006;**96**:90–7.
24. Su W, Wei SS, Hu SQ, Tang JX. Preparation of TiO_2/Ag colloids with ultraviolet resistance and antibacterial property using short chain polyethylene glycol. *J Hazard Mater* 2009;**172**:716–20.
25. Yuranova T, Rincon AG, Pulgarin C, Laub D, Xantopoulos N, Mathieu H-J, et al. Performance and characterization of Ag–cotton and Ag/TiO_2 loaded textiles during the abatement of *E. coli*. *J Photochem Photobiol A: Chem* 2006;**181**:363–9.
26. Ma C-M, Ku Y, Kuo Y-L, Chou Y-C, Jeng F-T. Effects of silver on the photocatalytic degradation of gaseous isopropanol. *Water Air Soil Pollut* 2009;**197**:313–21.